Environmental Science and Pollution Research (2025) 32:23810–23819
https://doi.org/10.1007/s11356-024-32861-6

RECENT ADVANCES IN DECARBONIZATION TECHNOLOGIES FOR SUSTAINABLE DEVELOPMENTS

Experimental investigation of diethyl ether (DEE) blended jack fruit peel oil (JFP) with hydrogen as a secondary fuel in dual-fuel compression ignition engines

Mahesh Rajasekaran[3] · Sangeetha Krishnamoorthi[1] · Mathanraj Vijayaragavan[2]

Received: 11 October 2023 / Accepted: 7 March 2024 / Published online: 19 March 2024

Abstract

Jack fruit peel oil (JFPO) exhibits passive chemical characteristics; thereby, dual-fuel mode frequently involves hydrogen to address its combustion difficulties. This strategy has been gaining prominence nowadays. The present investigation investigates on the performance, emission, and combustion characteristics of a direct injected compression ignition dual-fuel engine operating on a binary fuel blend of jack fruit peel oil (JFPO) and diethyl ether with hydrogen induction. The engine was operated by inducing hydrogen gas into the intake manifold of the engine at 8 and 10 LPM with the applied load ranging from 25 to 100%. The test fuel was prepared by blending jack fruit peel oil and diethyl ether in the volumetric ratio of 90:10. JFP brake thermal efficiency was 16% lower than diesel at full load but enhanced by 9% with direct hydrogen induction at a knock limit of 10 LPM and 23% with JFP + H_2 + 10% DEE at maximum load. At maximum load, JFP + 10 LPM of hydrogen gas + 10% DEE produces 916 ppm of NO_x, which is 44.46% less than diesel. Furthermore, adding hydrogen gas and DEE to air fuel mixture decreased emissions of carbon monoxide and unburned hydrocarbon by 0.702% and 28.30% opa, respectively.

Keywords Carbon emission · Jack fruit peel · Performance · Emission · Combustion

Nomenclature

ASTM	American Society for Testing and Materials
BP	Brake power
bTDC	Before top dead center
BTE	Brake thermal efficiency
CHNS/O	Carbon/hydrogen/sulfur analyzers
CI	Compression ignition
CIME	*Calophyllum inophyllum* Methyl ester
CIO	*Calophyllum inophyllum* Oil
CNG	Compressed natural gas
CNT	Carbon nanotube
CO	Carbon monoxide
CO_2	Carbon dioxide
CSO	Cotton seed oil
DEE	Diethyl ether
GC-MS	Gas chromatography–mass spectrometry
GHG	Greenhouse gas
H_2	Hydrogen gas
HC	Hydrocarbon
JFPO	Jack fruit peel oil
kW	Kilowatt
LPG	Liquefied petroleum gas
LPM	Liters per minute
NDIR	Non-dispersive infrared
NO_x	Oxides of nitrogen
OH	Hydroxide
Opa	Opacity
PM	Particulate matter
ppm	Parts per million
UHC	Unburnt hydrocarbon

Responsible Editor: Philippe Garrigues

✉ Mathanraj Vijayaragavan
mathanraj.srm@gmail.com

[1] Department of Mechanical Engineering, Aarupadai Veedu Institute of Technology, Chennai 603104, India

[2] Department of Mechanical Engineering, Faculty of Engineering and Technology, SRM Institute of Science and Technology, Kattankulathur 603203, India

[3] Department of Mechanical Engineering, Vinayaka Missions Research Foundation, Chennai 603104, India

Introduction

Extensive research into clean, sustainable, technically feasible, compatible, and universally acceptable energy resources has been driven by rising energy demand, the inadequacy of traditional fuels, soaring energy prices, and environmental concerns arising from the exploitation of petroleum fuels (Soudagar et al. 2019). Hazardous emissions, including organic compounds that pose dangers to human health including naphthalene, formaldehyde, benzene, acetaldehyde, and acrolein, have significantly increased as a result of the boom in the use of conventional fuels (Saxena et al. 2017). As a result, significant efforts have been made to lessen the negative effects of conventional fuels on the environment.

The durability, high compression ratio, low fuel cost, high thermal efficiency, and low maintenance costs of compression ignition (CI) engines are well-liked; however, they are associated with harmful exhaust pollutants (CO, CO_2, NO_x, PM, UHC, soot, acrolein, and formaldehyde) (Ospina et al. 2019), with NO_x being a major concern (Ospina et al. 2019; Chen et al. 2019). Energy research efforts in the recent past have focused on low-NO_x methods development, using two primary strategies: (1) replacing conventional fuels with LPG, CNG, biodiesel, and hydrogen fuel (Ashok et al. 2018) and (2) adding additives to improve burning rates and lower emissions (Dinesha et al. 2019; Senthil et al. 2019). The favorable qualities of biodiesel and hydrogen gas, such as their appropriate oxygen content, sulfur-free composition, ease of production, low greenhouse gas emissions, and clean combustion, have made them the focus of current study (Tayari and Abedi 2019).

There is an increasing need for resources because the transportation industry uses two thirds of all energy derived from natural resources. Overpopulation, industrialization, and urbanization have increased demand, which has led to pollution and other environmental problems (Manigandan et al. 2021). Carbon footprints, global warming, and higher temperatures are all caused by pollution. A move towards clean, eco-friendly, commercially feasible, and energy-efficient fuel substitutes is required to meet these issues (Boomadevi et al. 2021). Since biodiesel satisfies each of these requirements, it is clearly a promising substitute. When compared to normal petrol, biodiesel promotes environmental purity, ease of storage, and less engine modification because it uses organic materials rather than fossil fuels. It is often obtained from recyclable renewable resources (Jjagwe et al. 2021; Van Gerpen et al. 2007). Researchers like Igbokwe and Nwafor (2016) used Nigerian palm kernel oil, Mostafa and El-Gendy (2017) examined the fuel qualities of microalga *Spirulina platensis* for use in internal combustion engines, and Avulapati et al. (2016) used biodiesel in addition to conventional fuel. The invention of vegetable oils as a new fuel source for motors by Rudolf Diesel in 1895 gave rise to biodiesel. The bulk of vegetable oils used in engines include saturated hydrocarbons (Meher et al. 2006; Kesharvani et al. 2023; Barnwal and Sharma 2005).

Nanthagopal et al. (2018) and Tiwari et al. (2021) observed that biodiesel blends improved engine performance by increasing brake thermal efficiency and decreasing hydrocarbon (HC) and NO_x emissions. Additionally, Lee and Kim (2017), Thodda et al. (2023), Rajpoot et al. (2023), and Ramasamy et al. (2023) investigated alternate fuels and catalysts, showing the potential of diethyl ether and acetylene in boosting engine efficiency and lowering emissions. Soetardji et al. (2014) performed extensive research on jack fruit peel, highlighting its potential as a raw material for biofuel generation. The peel was collected from a jack fruit chip manufacturer in East Java, Indonesia, and subjected to a variety of assays, including ultimate and proximate analysis, as well as ASTM-based heating value calculation. The pursuit of sustainable and ecologically friendly energy sources has resulted in substantial study into alternative fuels, with biodiesel emerging as a promising option. The studies presented in this article illustrate the potential of biodiesel and other alternative fuels to improve engine performance while lowering harmful emissions, resulting in a cleaner and more sustainable transportation sector.

Objective of the study and fuel preparation

The primary objective of this investigation is to explore the possibilities of using CI engine petrol and jack fruit peel oil as a sustainable feedstock for biodiesel. Owing to the peel oil's poor combustion properties, the traditional method entails trans-esterifying it into biodiesel; however, this study investigates an alternative by combining 10% by volume of diethyl ether (DEE), an oxygenated additive, with jack fruit peel oil. The purpose of the study is to assess how different loads affect engine performance, combustion, and emissions in relation to hydrogen induction. Table 1 shows the standards used for the measurement of properties. The investigation's uniqueness pertains in its emphasis on the synergistic benefits of hydrogen induction and an oxygenated ingredient, DEE, when combined with jack fruit peel oil. While prior studies focused mostly on trans-esterification of peel oil to biodiesel, this study takes a novel strategy, investigating the effects of combining an oxygenated additive with hydrogen enrichment. The study's original component is its potential to improve engine characteristics using an innovative combination of hydrogen and an DEE in a combustion engine (CI) operating on jack fruit peel oil.

Table 1 ASTM standards used for determination of fuel properties

Property	Test standards	Biodiesel standards		
		ASTM D6751-15c	EN 14214/14213	Method
Kinematic viscosity, cST at 40 °C	ASTM D445	1.9–6.0	3.5–5.0	Redwood viscometer
Density at 15 °C, g/cm^3	ASTM D1298	-	0.860–0.900	Pycnometer
Lower heating value, kJ/kg	ASTM D240	-	Min 35,000	Bomb calorimeter
Cetane index	ASTM D976	Min 47	Min 51	Calculated based on API gravity and mid-boiling point
Flashpoint, °C	ASTM D93	Min 93	Min 120	Pensky Martens apparatus (closed cup)

Table 2 Properties of diesel, jack fruit peel oil, diethyl ether, and hydrogen

Fuel properties	Diesel	Jack fruit peel oil	Diethyl ether	Hydrogen
Density at 35 °C (kg/m^3)	830	1200	713	0.08
Lower heating value (MJ/kg)	42.5	29.3	33.2	120
Viscosity (cST)	4	31.8	0.33	-
Cetane number	45	52	< 125	-

Experimental setup

Hydrogen induction system

The engine was operated in the dual-fuel mode using 99.99 percent pure industrial hydrogen. Table 2 details the characteristics of hydrogen fuel. A hydrogen induction input system was developed, comprising a hydrogen gas cylinder, dry and wet flame arrestors, a fuel flow meter, and a venturi. A two-stage pressure regulator in the induction system reduced hydrogen cylinder pressure from 220 to 1.5 bar for usage in the engine. Wet flame arrestors are filled with 1/3 pint of water, and regulator-fed hydrogen gas passes through these. On the other hand, hydrogen is provided via a dry flame arrestor. Two flame arrestors are used to prevent flashback from occurring during hydrogen combustion. Figure 1 represents the schematic diagram of hydrogen supply system.

Test rig

A Kirloskar single-cylinder, water-cooled, four-injection, naturally aspirated diesel engine generating 5.2 kW of power at 1500 rpm was used during all experiments. Table 3 provides the technical details, and Fig. 2 depicts the experimental set-up's construction. The engine was linked up to an electrically powered eddy current dynamometer for load monitoring and

Table 3 Engine specifications

Make and model	Kirloskar TV1
Engine type	Single-cylinder, water-cooled, direct injection, constant speed
Bore (mm)	87.5
Stroke (mm)	110
Compression ratio	17.5:1
Rated power at 1500 rpm	5.2 kW
Injection pressure (bar)	200
Injection timing	23°bTDC
Number of injector nozzle holes	3
Nozzle diameter	0.280 mm
Injection pressure	210 bar
Control mechanism	Governor
Piston geometry	Hemispherical

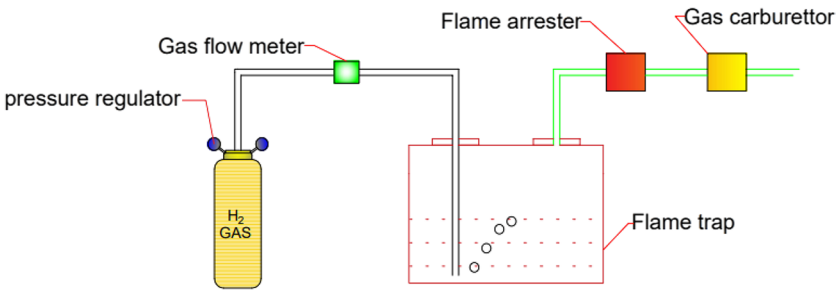

Fig. 1 Hydrogen supply system

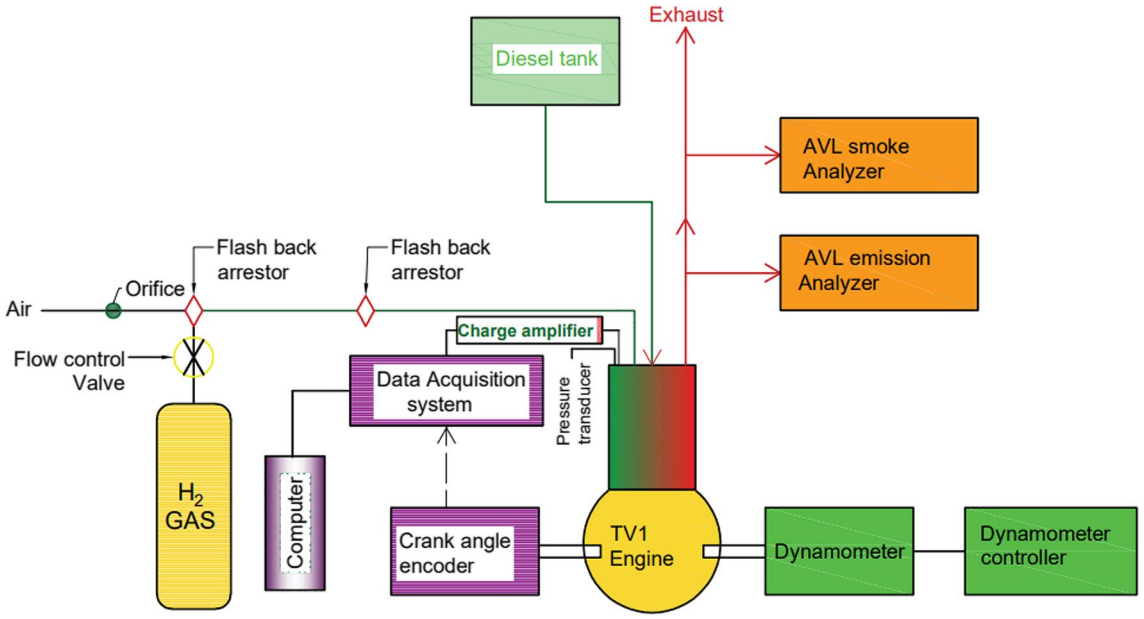

Fig. 2 A schematic representation of the experimental setup

adjustment. A burette and timer were used to track volumetric fuel consumption, while a type K thermocouple with a digital display was used to detect exhaust gas temperature. Emissions of HC, NO_x, CO_2, and CO were measured with an AVL di-gas 444 model analyzer equipped with non-dispersive infrared (NDIR) technology. An AVL 437C-type opacimeter was used to measure smoke opacity via light extinction. The calibration of gas analyzers was done before the experiment. Crank angle was recorded by flywheel encoders, and cylinder pressure was collected by Kistler pressure gauges that were integrated with computerized data collection systems. The 'Engine Soft' program computed the in-cylinder pressure, heat release rate, ignition delay, and combustion duration. Data were collected over 100 cycles and the average was calculated to reduce cycle-to-cycle fluctuation. Table 4 describes the equipment accuracy and the uncertainty for this study. Brake power (BP) values of 1.3 kW, 2.6 kW, 3.9 kW, and 5.2 kW were used in all tests at 1500 rpm, ranging from low to high loads. Throughout the experiment, the direct injection pressure remained constant at 210 bar and the injection time was fixed to 23°bTDC. All testing were carried out without modifying the test engine. The parameters were determined using the average value of five measurements.

Fuel preparation and tests

The jack fruit peel was washed multiple times with tap water to get rid of organic materials and dirt preceding

Table 4 Ranges and measuring technique of various instruments

Measurement	Accuracy	% Uncertainty	Measurement technique
Load	±0.1 kg	±0.55	Strain gauge-type load cell
Speed	±1 rpm	±0.07	Magnetic pickup type
Burette fuel measurement	±0.1 cc	±1	Volumetric measurement
Time	±0.2 s	±0.2	Manual stop watch
Manometer	±1 mm	±1	Principle of balancing column of liquid
CO	±0.02%	±0.2	NDIR principle
HC	±20 ppm	±0.2	NDIR principle
CO_2	±0.03%	±0.15	NDIR principle
NO	±10 ppm	±1	Electrochemical measurement
Smoke	±1% opacity	±1	Opacimeter
EGT indicator	±1 °C	±0.15	K-type thermocouple
Pressure pickup	±0.5 bar	±1	Piezoelectric sensor
Crank angle	±1°	±0.2	Magnetic pickup type

utilizing. After cleaning, the jack fruit peel was oven-dried at 100 °C for 24 h to reach a moisture content of 5%. After drying, the jack fruit peel was finely powdered to 80/100 mesh. The ultimate analysis of the jack fruit peel was performed using a Perkin-Elmer 2400 CHNS/O elemental analyzer, while normal ASTM protocols were used for proximate analysis, which included water, ash, and volatile matter. The ultimate examination of the jack fruit peel was performed using a Perkin-Elmer 2400 CHNS/O elemental analyzer, while normal ASTM protocols were used for proximate analysis, which included water, ash, and volatile matter. The fixed carbon content was calculated by subtracting the percentages of moisture, ash, and volatile matter from 100%. The heating value of the jack fruit peel was determined to be 17.9 MJ/kg using the ASTM procedure D5865-12 in an oxygen bomb calorimeter. The different combinations of fuels used for testing are (1) JFP100 — jack fruit peel biodiesel, (2) JFP100 + H_2 — jack fruit peel biodiesel with hydrogen induction (8 and 10 LPM), and (3) JFP100 + 10 LPM H_2 + 10% DEE — jack fruit peel biodiesel blended with DEE and hydrogen induction as secondary fuel. The fuel properties are shown in Table 2.

The experimental analysis was conducted in a single-cylinder water-cooled diesel engine. The engine was made to operate at 4 different load conditions with the load interval of 25%. Hydrogen gas was inducted into the manifold at 8 and 10 LPM, respectively. In order to improve the reactivity of the fuel DEE was directly blended with the test fuel with 10% on volumetric basis. The jack fruit peel oil without being trans-esterification was used a direct injected fuel in this analysis. The mixing ratio and the hydrogen gas flow rate were selected based on the existing literature survey. A clear and through uncertainty analysis was conducted to determine the repeatability/uncertainty error percentage of the experimental analysis which is shown in Table 4 and 5.

Table 5 Uncertainty of various parameters

Parameters	% Uncertainty
Brake power	±0.55
Brake thermal efficiency	±0.334
Brake-specific energy consumption	±1.13
CO_2 emission	±1.45
NO emission	±1.75
Smoke opacity	±1
HC emissions	±1.45
CO emission	±1.45

Performance analysis

Brake thermal efficiency

Figure 3 shows how the BTE changes for diesel engines with different loads: JFP100, JFP100 with hydrogen induction (8 and 10 LPM), and JFP100 plus 8 LPM H_2 + 10% DEE. When the engine is at its max load, the BTE for diesel is found to be 30.31%, while the BTE for JFP100 is found to be 24.45%. Different physical properties of JFP100 led to an inefficient burning process, which led to a lower BTE. Because hydrogen burns quickly and has a high calorific value, knock-limited hydrogen and JFP100 showed increased efficiency work well together. The performance of JFP100 + 10 LPM H_2 + 10% DEE was much better than adding hydrogen or using clean JFP100. At full load, the BTE for JFP100 + 10 LPM H_2 + 10% DEE was raised to 31.2%, which is higher than diesel at full load. This could be because it has much better physical qualities, like a much higher cetane index and less density and viscosity (Thangavel et al. 2023). All of these things led to better results from the DEE addition.

Brake-specific energy consumption

Diesel engine, JFP100, JFP100 with hydrogen induction (8 LPM and 10 LPM), and JFP100 + 10 LPM H_2 + 10% DEE were all tested for their brake-specific energy consumption (BSEC) under varying loads, as shown in Fig. 4. Diesel has a BSEC of 11.87 MJ/kWh, while JFP100 BSEC is 14.14 MJ/kWh. Since JFP100 has a lower calorific value and a higher viscosity, it burns less efficiently, leading to higher fuel consumption. Since hydrogen has a larger calorific value and the flame speed of JFP100 hydrogen induction is increased,

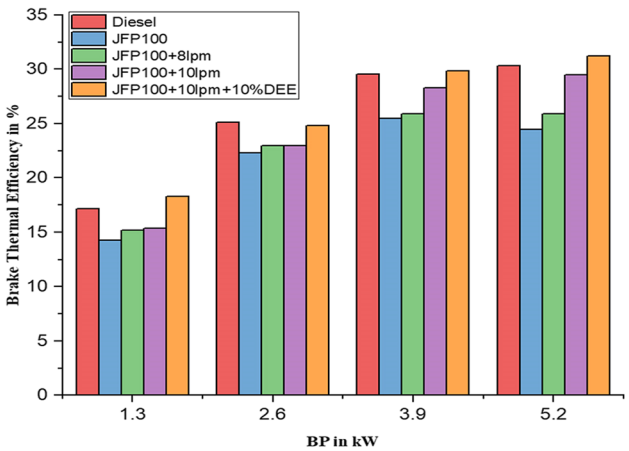

Fig. 3 BTE for CASO, CASO + H_2, and CASO + H_2 + DEE at full load

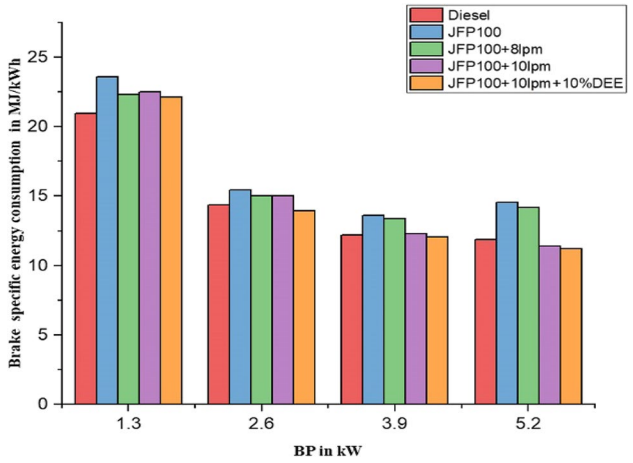

Fig. 4 BSEC for CASO, CASO + H_2, and CASO + H_2 + DEE at full load

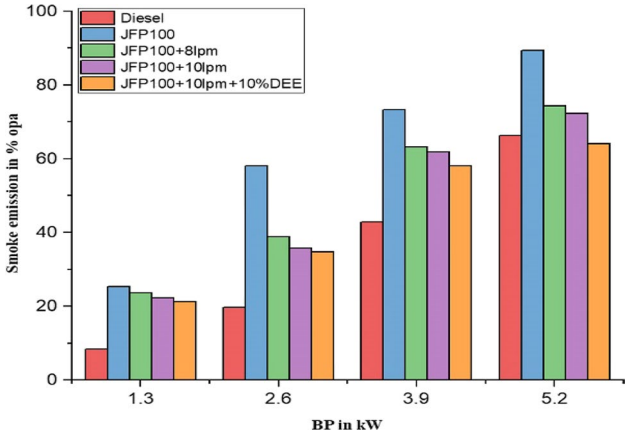

Fig. 6 Smoke emissions for CASO, CASO + H_2, and CASO + H_2 + DEE at full load

the same amount of power can be generated with less fuel. Improved combustion is indicated by a lower BSEC for JFP100 + H_2 at 10 LPM (11.41 MJ/kWh) compared to JFP100. By adding DEE in the future, JFP100 + 10 LPM H_2 will have better physical properties and burn more efficiently than diesel (Yusri et al. 2019).

Emission parameters

Oxide of nitrogen

Figure 5 shows the NO_x emissions of diesel, JFP100, JFP100 with different amounts of hydrogen added, and JFP100 + 10 LPM H_2 + 10% DEE under different loads. NO_x fumes are caused by too much oxygen and a high temperature during combustion. At full load, diesel emissions are 1698 ppm and JFP100 emissions are 1329 ppm. Low NO_x emissions are caused by the fact that JFP100 does not burn well, which makes it burn at a lower temperature because it does not produce as much heat overall. NO_x output went up to 1720 ppm at full load after hydrogen was added. Hydrogen has a high calorific value, so it raises the temperature of burning. This makes more NO emissions, which is indigent. Also, because hydrogen has a low cetane index, it takes longer to flame propagation, which means it gives off more NO. Also, when DEE was added to JFP100, the amount of NO emissions was even lower than with diesel and JFP100. This could be because JFP100 fuel contains DEE, which has a higher auto-ignition temperature and is more volatile, so it chooses a shorter ignition delay effect during combustion. At full load, the JFP100 + 10 LPM H_2 + 10% DEE has 916 ppm of NO_x pollution, which is about 46.05% less than diesel (Subramanian et al. 2020). An upsurge in the temperature of exhaust gases generally results in higher NO_x emissions because it improves the combustion process and promotes the generation of nitrogen oxides. When 10 L per minute (LPM) of hydrogen and diethyl ether is added to the combustion process, some impacts on NO_x emissions can be seen. Hydrogen, as a high-octane fuel, burns at greater temperatures, thus raising the EGT and thus boosting NO_x emissions. Diethyl ether, on the other hand, has distinct combustion properties that may impact combustion chemistry and counterbalance temperature rise, thereby decreasing NO_x generation. Understanding the relationship between exhaust gas temperature and the addition of hydrogen and diethyl ether is critical for optimizing combustion processes and reducing environmental effect (Soudagar et al. 2018).

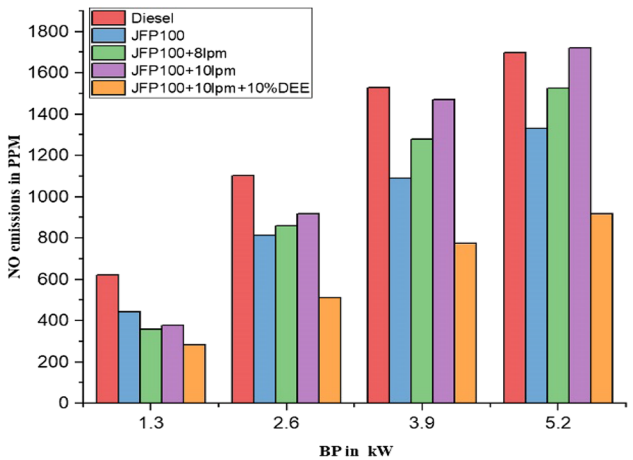

Fig. 5 NO_x emissions for CASO, CASO + H_2, and CASO + H_2 + DEE at full load

Smoke emissions

Soot formed in the exhaust as fuel was injected up until the diffusion combustion phase. Different test fuels and loads

appear to account for the various degrees of smoke opacity depicted in Fig. 6. At full throttle, the smoke opacity of diesel is 66.2% opa, while that of JFP100 is 89.3% opa. According to the results of the JFP100 study, increased smoke emission is the result of lower quality physical characteristics, such as greater density and viscosity, which lead to inefficient molecular breakdown during burning and the subsequent generation of soot particles. Hydrogen reduces smoke opacity by 28.30% compared to JFP100. Hydrogen gas, being a carbon-free fuel, helps reduce smoke emissions. Hydrogen, when combined with a high combustion temperature, aids in the oxidation of the unburned soot particles in the combustion chamber, leading to less smoke opacity in the exhaust. With JFP100 + 10 LPM H_2 + 10% DEE, smoke opacity was slightly reduced compared to JFP100. Although JFP100 + 10 LPM H_2 + 10% DEE improved performance, the shorter stage of premixed combustion caused by the higher cetane index of a fuel resulted in slightly less smoke opacity (Muthukumaran et al. 2015). The fuel higher cetane index accounted for this. One possible explanation is because DEE has too many oxygen atoms.

HC emission

In a CI engine, many things can happen at the same time, such as burning, mixing of burned and unburned gas, fuel injection, evaporation, mixing of fuel and air, and atomization. HC fumes were made when fuel was burned for many different reasons. Most hydrocarbon fumes come from cooling the cylinder walls and not mixing the fuel well enough. Hydrocarbon gas that has not been burned and is stuck in the cracks of the engine cylinder is another source of HC fumes. Figure 7 shows the HC emissions for gasoline, JFP100, JFP100 with different amounts of hydrogen added, and JFP100 + 10 LPM H_2 + 100% DEE at different loads. When both diesel and JFP100 are running at full power, they put out 75 and 122 ppm of HC, respectively. Because JFP100 is thicker and denser, it makes the mixture of fuel and air less efficient, which makes more hydrocarbons (HC) than other fuels. Also, the quench distance is longer because JFP100 causes poor combustion, which stops the spark from spreading to the cylinder walls. Because hydrogen has a faster flame speed, adding hydrogen is a good way to speed up burning. Because hydrogen burns faster, adding it to a fire makes it burn better. With the help of hydrogen, the flame can get closer to the cylinder sides. This cuts down on the distance it takes to put out the flame and the amount of HC that is released. The least amount of HC was released by JFP100 + 10 LPM H_2 + DEE10. Because the cetane index and other physical properties have gotten better, HC emissions have gone down. With JFP100 + 10 LPM H_2 + DEE10, oxidizing unburned HC emissions is helped by a higher burning temperature (Martin et al. 2012).

CO emissions

CO emissions vary for diesel, JFP100, and JFP100 with variable hydrogen induction as shown in Fig. 8. The combustion process generates a certain quantity of CO as an intermediate species, and this amount is proportional to the air-to-fuel ratio. Combustion in CI engines is facilitated by a large quantity of oxygen thanks to the aspiration of air that happens naturally in these engines. This helps explain why CI engines, compared to gasoline engines, will produce less carbon monoxide. Diesel has a 0.164% vol CO emission rate, while JFP100 rate is 1.165%. Incomplete combustion is possible due to JFP100 poor physical properties, such as its high density and viscosity, which increase CO production. Low combustion temperatures, the result of poor combustion, delay CO oxidation. The volume of carbon monoxide

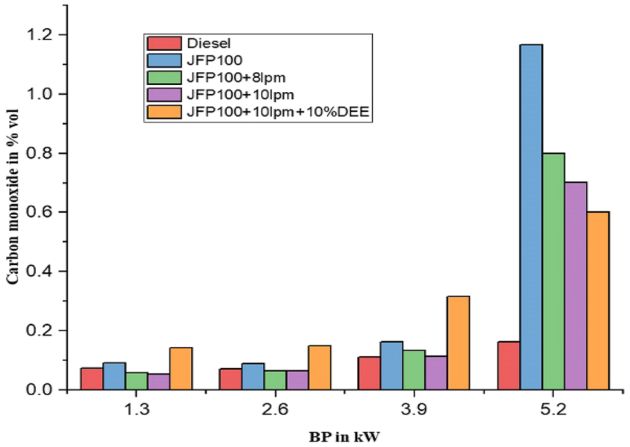

Fig. 7 HC emission for CASO, CASO + H_2, and CASO + H_2 + DEE at full load

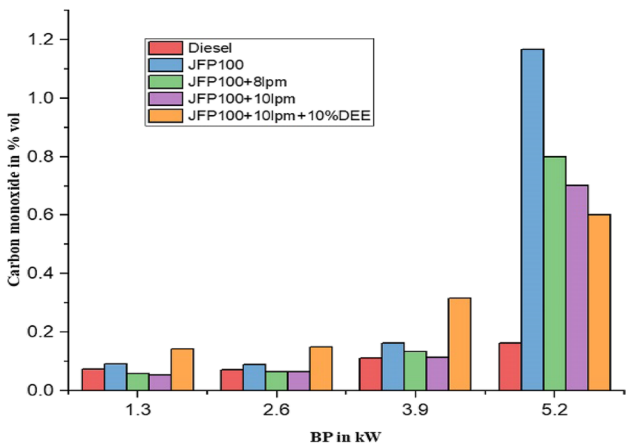

Fig. 8 CO emissions for CASO, CASO + H_2, and CASO + H_2 + DEE at full load

emissions has dropped to a historic low of 0.702% vol for JFP100 + H_2. Hydrogen absence of carbon and its ability to improve combustion made this reduction achievable. At greater combustion temperatures, the intermediate species CO is transformed to carbon dioxide. However, hydrogen induction dilutes incoming air, reducing available oxygen.

CO emissions for JFP100 + 10 LPM H_2 + 10% DEE at maximum load is 0.60% volume due to hydrogenation improved fuel properties. We improved combustion over direct hydrogen induction by increasing density and viscosity.

Combustion characteristics

Figure 9 shows that the peak pressure for diesel, JFP100, JFP100 with hydrogen induction (8 and 10 LPM), and JFP100 + 10% DEE + 10 LPM are 68.48, 67.39, 68.16, 72.04, and 74.25 bar. The decreased value for JFP100 is due to poor physical properties.

Hydrogen induction lowers air temperature, extending ID. The extended ID period allows fuel more time to prepare for combustion, which is the only cause of peak pressure rise. JFP100 peak hydrogen energy sharing pressure around 72.04 bar. In comparison to diesel, JFP100 + 10% DEE + 10 LPM hydrogen has the highest peak pressure. DEE in fuel increases peak pressure because hydrogen has a better heating value and DEE has high self-ignition temperature.

Figure 10 shows that the HRR for diesel, JFP100, JFP100 with hydrogen induction (8 and 10 LPM), and JFP100 + 10% DEE + 10 LPM are 65°J/CA, 59°J/CA, 65°J/CA, 70°J/CA, and 72.5°J/CA. Due to inadequate fuel preparation during combustion, JFP100 has a lower HRR than diesel. Biofuel's viscosity, density, and lower heating value affect fuel preparation. Lower HRR raises

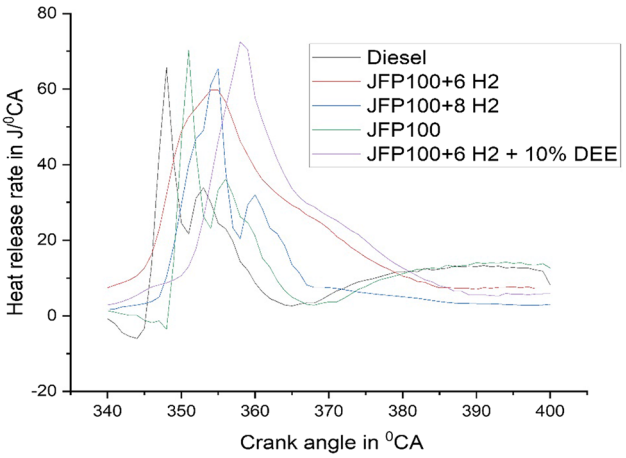

Fig. 10 HRR for CASO, CASO + H_2, and CASO + H_2 + DEE at full load

BSFC, reducing brake power. Figure 10 indicates that hydrogen raises the HRR and will continue to raise it for DEE fuel with hydrogen. This is due to hydrogen's longer ID and fast flame velocity. The higher HRR in premixed combustion raises combustion chamber temperature, increasing NO emissions as shown in the NO emission (Deshwar et al. 2023).

A comparison of the ignition delay and combustion duration for diesel, JFP100, JFP100 with hydrogen induction (8 and 10 LPM), and JFP100 + 10% DEE + 10 LPM is shown in Fig. 11. The ID is located between the injection and combustion processes. There are two phases to identification: chemical lag time and physical delay, which includes the process of preparing fuel for combustion and igniting it automatically. In the case of DEE mixed fuel, the ID period is continuously evolving with 10 LPM hydrogen gas; it is somewhat increased compare to JFP100. ID values of 12°CA

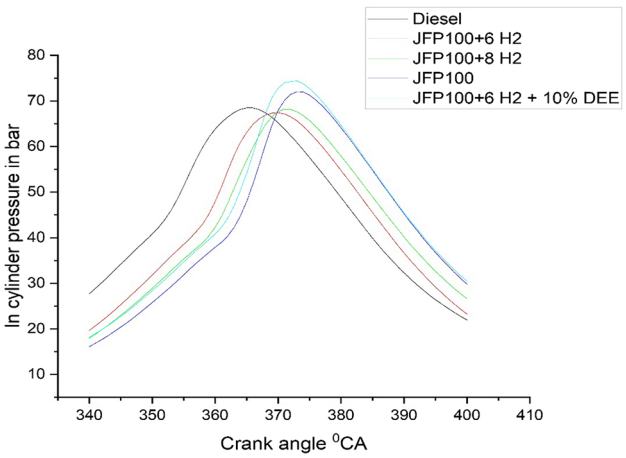

Fig. 9 Peak pressure for CASO, CASO + H_2, and CASO + H_2 + DEE at full load

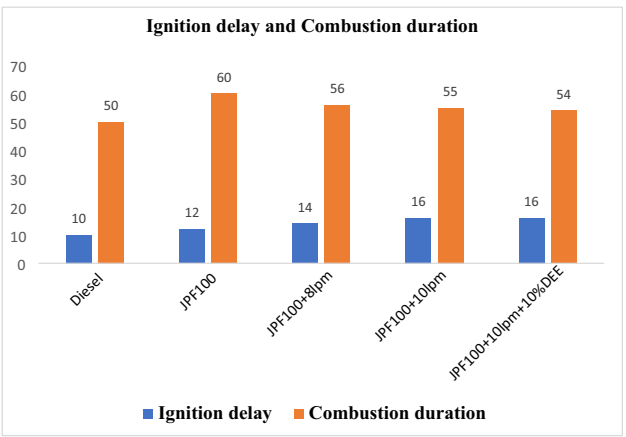

Fig. 11 ID and CD for CASO, CASO + H_2, and CASO + H_2 + DEE at full load

and 10°CA are assigned to JFP100 and diesel when they are fully fueled, respectively.

Figure 11 shows the CD for diesel, JFP100, JFP100 with hydrogen induction (8 and 10 LPM), and JFP100 + 10% DEE + 10 LPM. CD is primarily affected by air and fuel injection. Regionally produced fuel–air combinations that are rich oxidize at a slower rate. Both diesel and JFP100 with hydrogen induction (10 LPM) have a combustion time of 55 °C. In addition to increasing the rates of JFP100 with hydrogen induction (10 LPM) combustion, fuel spray features also improve diffusion combustion. The addition of DEE to pilot fuel at a volume of 10% resulted 54°CA is decreased compared to JFP100 with hydrogen induction (10 LPM), respectively. The combustibility of hydrogen and DEE helps to reduce CD because high flame speed, quenching distance, flame fronts, and octane number all contribute to a reduction in the amount of time required for combustion.

Conclusions

In this study, the use of JFP100 oil as a primary fuel alternative for petrol was investigated. Hydrogen was added by mixing and induction, and DEE was added as an additive to improve the overall performance. The study sought to determine the engine's performance, emissions, and combustion characteristics. The further investigation produced the following observations:

1. Brake thermal efficiency: JFP100 exhibited lesser brake thermal efficiency than diesel; however, the introduction of hydrogen in DEE improved efficiency. Specifically, JFP100 + 10 LPM H_2 + 10% DEE outperformed JFP100 + 10 LPM H_2 + 10% DEE.
2. Hydrogen addition impact: Adding hydrogen to DEE-mixed fuel accelerated and improved combustion, resulting in lower fuel usage.
3. Emission characteristics: JFP100 had lower NO_x emissions than petrol but produced more smoke. The injection of hydrogen reduced smoke output, but with an increase in NO_x levels. JFP100 + 10 LPM H_2 + 10% DEE, with a high cetane number, emits less NO_x.
4. Hydrocarbon (HC) and carbon monoxide (CO) emissions: Compared to the base fuel, JFP100 + 10 LPM H_2 + 10% DEE had lower HC and CO emissions.
5. Ignition delay: JFP100 showed a larger delay in starting than JFP100 with hydrogen induction. JFP100 + 10 LPM H_2 + 10% DEE, with its high cetane index, has the shortest igniting delay.

The findings of these studies highlight the possibility for increasing JFP100 combustion and operational efficiency by adding and combining hydrogen with DEE. In terms of efficiency and pollution management, a JFP100 + 10 LPM H_2 + 10% DEE engine performed better than a direct hydrogen induction CI engine. Using JFP100 in CI engines without going through the trans-esterification process, the dual-fuel method and blending approach provide a feasible alternative.

Future scope of work

More research could be done to improve performance by adding alcohol and an after-treatment device so that emission parameters can go down in the future.

Author contribution Magesh prepared the manuscript with the relevant data. The final manuscript was corrected and verified by Dr. Sangeetha Krishnamoorthi and Dr. Mathanraj Vijayaragavan. Further, all authors read and approved the final manuscript for submission.

Data availability All the research data used in the study are available in the manuscript.

Declarations

Ethics approval The research did not involve human or animal participants, and there was no release of harmful substance to the environment as a result of the study. The authors followed the rules for good scientific practice, as described in the author guidelines.

Consent to participate Not applicable, as there were no human participants in the study.

Consent for publication I, the undersigned, give my consent for the publication of identifiable details, which can include photograph(s) and/or videos and/or case history and/or details within the text ("Material") to be published in the above Journal and Article.

Competing interests The authors declare no competing interests.

References

Ashok B, Nanthagopal K, SakthiVignesh D (2018) *Calophyllum inophyllum* methyl ester biodiesel blend as an alternate fuel for diesel engine applications. Alexandria Eng J 57:1239e47. https://doi.org/10.1016/j.aej.2017.03.042

Avulapati MM, Ganippa LC, Xia J, Megaritis A (2016) Puffing and micro-explosion of diesel–biodiesel–ethanol blends. Fuel 166:59–66. https://doi.org/10.1016/j.fuel.2015.10.107

Barnwal B, Sharma M (2005) Prospects of biodiesel production from vegetable oils in India. Renew Sust Energ Rev 9(4):363–378. https://doi.org/10.1016/j.rser.2004.05.007

Boomadevi P, Paulson V, Samlal S, Varatharajan M, Sekar M, Alsehli M et al (2021) Impact of microalgae biofuel on microgas turbine aviation engine: a combustion and emission study. Fuel 302:121155. https://doi.org/10.1016/j.fuel.2021.121155

Chen X, Wang Z, Pan S, Pan H (2019) Improvement of engine performance and emissions by biomass oil filter in diesel engine. Fuel 235:603e9. https://doi.org/10.1016/j.fuel.2018.08.038

Deshwar P, Kumar G, Subramanian B, Panchal SH, Thangavel V, Ismail S, Feroskhan M (2023) Simultaneous reduction of NO_x and smoke emissions in gasoline-ethanol blended RCCI engine with biogas as a ternary fuel. Int J Energy Clean Environ 24(2). https://doi.org/10.1615/InterJEnerCleanEnv.2022040767

Dinesha P, Kumar S, Rosen MA (2019) Combined effects of water emulsion and diethyl ether additive on combustion performance and emissions of a compression ignition engine using biodiesel blends. Energy 179:928e37. https://doi.org/10.1016/j.energy.2019.05.071

Igbokwe JO, Nwafor OMI (2016) Performance characteristics of palm kernel biodiesel and its blend in a CI engine. Int J Ambient Energ 37(1):103–106. https://doi.org/10.1080/01430750.2014.897647

Jjagwe J, Olupot PW, Menya E, Kalibbala HM (2021) Synthesis and application of granular activated carbon from biomass waste materials for water treatment: a review. J Bioresour Bioprod. https://doi.org/10.1016/j.jobab.2021.03.003

Kesharvani S, Dwivedi G, Verma TN (2023) Optimization of performance characteristics in diesel engine utilizing *Chlorella vulgaris* fuel—a green approach towards sustainable development. Environ Sci Pollut Res. https://doi.org/10.1007/s11356-023-27310-9

Lee S, Kim TY (2017) Performance and emission characteristics of a DI diesel engine operated with diesel/DEE blended fuel. Appl Therm Eng 121:454–461. https://doi.org/10.1016/J.APPLTHERMALENG.2017.04.112

Manigandan S, Gunasekar P, Praveen Kumar TR, Alahmadi TA, Subramanian N, Pugazhendhi A et al (2021) Influence of dynamic position, fluid intake, hydration, and energy expenditure on sustainable mobility transport. Appl Acoust 175:107809. https://doi.org/10.1016/j.apacoust.2020.107809

Martin MLJ, Edwin Geo V, KingslyJeba Singh D, Nagalingam B (2012) A comparative analysis of different methods to improve the performance of cotton seed oil fuelled diesel engine. Fuel 102:372–378. https://doi.org/10.1016/J.FUEL.2012.06.049

Meher L, Dharmagadda VS, Naik S (2006) Optimization of alkali-catalyzed transesterification of *Pongamia pinnata* oil for production of biodiesel. Bioresour Technol 97(12):1392–1397. https://doi.org/10.1016/j.biortech.2005.07.003

Mostafa SS, El-Gendy NS (2017) Evaluation of fuel properties for microalgae *Spirulina platensis* bio-diesel and its blends with Egyptian petro-diesel. Arab J Chem 10:S2040–S2050. https://doi.org/10.1016/j.arabjc.2013.07.034

Muthukumaran N, Saravanan CG, Prasanna Raj Yadav S, Vallinayagam R, Vedharaj S, Roberts WL (2015) Synthesis of cracked *Calophyllum inophyllum* oil using fly ash catalyst for diesel engine application. Fuel 155:68–76. https://doi.org/10.1016/J.FUEL.2015.04.014

Nanthagopal K, Ashok B, Saravanan B, Korah SM, Chandra S (2018) Effect of next generation higher alcohols and *Calophyllum inophyllum* methyl ester blends in diesel engine. J Clean Prod 180:50–63. https://doi.org/10.1016/J.JCLEPRO.2018.01.167

Ospina G, Selim MYE, Al Omari SAB, Hassan Ali MI, Hussien AMM (2019) Engine roughness and exhaust emissions of a diesel engine fueled with three biofuels. Renew Energy 134:1465e72. https://doi.org/10.1016/j.renene.2018.09.046

Rajpoot AS, Saini G, Chelladurai HM et al (2023) Comparative combustion, emission, and performance analysis of a diesel engine using carbon nanotube (CNT) blended with three different generations of biodiesel. Environ Sci Pollut Res. https://doi.org/10.1007/s11356-023-28965-0

Ramasamy SVM, Booramurthy V, Pandian S et al (2023) Synthesis and characterization of magnetic bifunctional nano-catalyst for the production of biodiesel from *Madhuca indica* oil. Environ Sci Pollut Res 30:66912–66922. https://doi.org/10.1007/s11356-023-26992-5

Saxena V, Kumar N, Saxena VK (2017) A comprehensive review on combustion and stability aspects of metal nanoparticles and its additive effect on diesel and biodiesel fuelled C.I. engine. Renew Sustain Energy Rev 70:563e88. https://doi.org/10.1016/j.rser.2016.11.067

Senthil R, Pranesh G, Silambarasan R (2019) Leaf extract additives: a solution for reduction of NO_x emission in a biodiesel operated compression ignition engine. Energy 175:862e78. https://doi.org/10.1016/j.energy.2019.03.039

Soetardji JP, Widjaja C, Djojorahardjo Y, Soetaredjo FE, Ismadji S (2014) Bio-oil from jackfruit peel waste. Procedia Chem 9:158–164. https://doi.org/10.1016/j.proche.2014.05.019

Soudagar MEM, Nik-Ghazali N-N, Kalam MA, Badruddin IA, Banapurmath NR, Akram N (2018) The effect of nano-additives in diesel-biodiesel fuel blends: a comprehensive review on stability, engine performance and emission characteristics. Energy Convers Manag 178:146e77. https://doi.org/10.1016/j.enconman.2018.10.019

Soudagar MEM, Nik-Ghazali NN, Kalam MA, Badruddin IA, Banapurmath NR, Yunus Khan TM et al (2019) The effects of graphene oxide nanoparticle additive stably dispersed in dairy scum oil biodiesel-diesel fuel blend on CI engine: performance, emission and combustion characteristics. Fuel 257:116015. https://doi.org/10.1016/j.fuel.2019.116015

Subramanian B, Venugopal T, Feroskhan M, Sivakumar R (2020) Emission characteristic of a dual fuel compression ignition engine operating on diesel + hydrogen & diesel + HHO gas with same energy share at idling condition. In IOP Conf Ser: Earth Environ Sci 573(1):012001. https://doi.org/10.1088/1755-1315/573/1/012001. (IOP Publishing)

Tayari S, Abedi R (2019) Effect of *Chlorella vulgaris* methyl ester enriched with hydrogen on performance and emission characteristics of CI engine. Fuel 256:115906. https://doi.org/10.1016/j.fuel.2019.115906

Thangavel V, Subramanian B, Ponnusamy VK (2023) Investigations on the effect of H_2 and HHO gas induction on brake thermal efficiency of dual-fuel CI engine. Fuel 337:126888. https://doi.org/10.1016/j.fuel.2022.126888

Thodda G, Kathapillai A, Madhavan VR et al (2023) Experimental analysis on the influence of compression ratio, flow rate, injection pressure, and injection timing on the acetylene — diesel aspirated dual fuel engine. Environ Sci Pollut Res 30:61217–61233. https://doi.org/10.1007/s11356-022-21483-5

Tiwari PK, Raj S, Kumar S, Singh P, Swaraj R, Sarkar S et al (2021) Influence of *Calophyllum inophyllum* and Jojoba oil methyl ester blended with *n*-pentanol additive upon overall performance, combustion and emission characteristics of a TDI engine operated in natural aspirated mode. Fuel 288:119576. https://doi.org/10.1016/J.FUEL.2020.119576

Van Gerpen JH, Peterson CL, Goering CE (2007) Biodiesel: an alternative fuel for compression ignition engines. American Society of Agricultural and Biological Engineers Kentucky, USA

Yusri IM, Mamat R, Akasyah MK, Jamlos MF, Yusop AF (2019) Evaluation of engine combustion and exhaust emissions characteristics using diesel/butanol blended fuel. Appl Therm Eng 156:209e19. https://doi.org/10.1016/j.applthermaleng.2019.02.028